Supplementary material

Boosting Photoelectrochemical Water Splitting: Enhanced Hole Transport in $BiVO_4$ Photoanodes via Interfacial Coupling

Hairu Wang[a], Yuying Bai[a], Rongling Wang[a], Yanan Fu[a], Qiong, Mei[c], Bo Bai[a], Qizhao Wang[a,b,*]

[a] School of Water and Environment, Key Laboratory of Subsurface Hydrology and Ecological Effects in Arid Region of Ministry of Education, Chang'an University, Xi'an 710054, Shaanxi, China

[b] College of Chemistry and Chemical Engineering, Northwest Normal University, Lanzhou 730070, Gansu, China

[c] School of Land Engineering, Chang'an University, Xi'an 710054, Shaanxi, China

*Corresponding author:

Qizhao Wang, E-mail: qzwang@chd.edu.cn, wangqizhao@163.com

Experimental Section

Text S1. Materials

$Co(CH_3COO)_2·4H_2O$、$Ni(NO_3)_2·6H_2O$、$(NH_4)_2Fe(SO_4)_2$、$Bi(NO_3)_3·5H_2O$、KI、KOH and anhydrous ethanol were purchased from Sinopharm Chemical Reagent Co., Ltd. P-benzoquinone (99.0%) and $VO(acac)_2$ were obtained from Shanghai Macklin Biochemical Technology Co., boric acid (H_3BO_3) and ammonia solution ($NH_3·H_2O$) was obtained from Tianjin Damao Chemical Reagent Factory.

Text S2. Preparation of nanoporous $BiVO_4$ photoanodes

$BiVO_4$ electrodes were prepared using a typical three-electrode electrodeposition method. First, $Bi(NO_3)_3·5H_2O$ (0.9701 g) was added to a solution (50 mL) containing 0.4 M KI (pH adjusted to 1.7). Next, 0.23 M p-benzoquinone ethanol solution (20 mL) was mixed with the above solution as the electrolyte used in the subsequent electrodeposition, in which a three-electrode system was used including a Pt counter electrode, an FTO glass working electrode, and an Ag/AgCl reference electrode. The BiOI membrane was obtained by fixing position of the CV electrode at a potential varying from -0.13 to 0 V, with a scanning rate of 5 mV/s. Then, the reddish brown BiOI membrane was obtained by washing with deionized water and dried. 180 μL of 0.2 M $VO(acac)_2$ DMSO solution was added dropwise to the prepared BiOI membrane and annealed at 450 °C for 2 h at a heating rate of 2 °C/min. Finally, the samples were immersed in 1.0 M NaOH solution to remove excess V_2O_5, then rinsed with distilled water and dried in an oven to obtain pure $BiVO_4$ electrode materials.

Text S3. Materials characterization

The microstructure of the samples was characterized by scanning electron microscopy (SEM, Sigma 300, ZEISS) and transmission electron microscopy (TEM, JEM-F200, JEOL). The elemental distribution of the samples was analyzed by energy spectrometry (EDS). X-ray diffraction (XRD) was recorded by Rigaku (D/max-IIIB, Japan) using Cu Kα as a radiation source. X-ray photoelectron spectroscopy (XPS) analysis of all samples was performed by an energy spectrometer (Thermo Scientific K-Alpha). The samples were characterized by UV-vis diffuse reflectance spectroscopy (UV-vis DRS) using a UV-vis spectrophotometer (U3010). The charge separation efficiency was analyzed by photoluminescence spectroscopy (PL, Hitachi F-4500).

Text S4. PEC measurements

PEC performance of photoanodes was evaluated in a standard three-electrode system (CHI 660e, Shanghai Chenhua Instruments Co., Ltd., China), containing photoanodes as working electrode, Ag/AgCl electrode (3.5 M KCl) as the reference electrode, and platinum as the counter electrode. A xenon lamp with an AM 1.5 G filter was used as the light source, and the light intensity was corrected to 100 mW cm^{-2} using a photopower meter. The PEC performance of the samples was evaluated in a rectangular quartz reactor (5 cm × 5 cm × 7 cm) using aqueous potassium borate (KBi, 1.0 M, pH = 9.5) as the electrolyte. Linear scanning voltammetry (LSV) was performed at a scan rate of 50 mV s^{-1} in a voltage window of -0.6 ~ 1.0 V vs. Ag/AgCl. Electrochemical impedance spectroscopy (EIS) was performed in the frequency range of 0.1 Hz to 100 kHz with 1.2 V vs. RHE as the initial voltage.

Incident photoelectric conversion efficiency (IPCE) measurements were performed at 1.23 V vs. RHE using a monochromator (71 SWS, Beijing Porphyry Technology Co., Ltd.) under AM 1.5G illumination. The precipitation of photoelectrochemical H_2 and O_2 was studied in 1.0 M KBi after 30 min of saturation with N_2 gas. Measurements were carried out by gas chromatography (GC-9560, Shanghai Huayi Chromatography Technology Co., Ltd.) based on standard H_2 and O_2 emission curves. All potentials were calibrated to the reversible hydrogen electrode (RHE) using the following equation.

$$E_{\text{vs. RHE}} = E_{\text{vs. Ag/AgCl}} + 0.059 \times \text{pH}$$

Text S5. Calculation of IPCE

Incident photon-to-current efficiency (IPCE) values were calculated using following equation:

$$IPCE(\%) = \frac{J \times 1240}{\lambda \times Plight} \times 100\% \quad (1)$$

Where J presents the photocurrent density ($mA \cdot cm^{-2}$) obtained from the electrochemical workstation. λ and P_{light} are the incident light wavelength (nm) and the power density obtained at a specific wavelength ($mW \cdot cm^{-2}$), respectively.

Text S6. Calculation of APCE

Absorption photon-current efficiency (APCE) can be calculated by the following equation:

$$APCE(\%) = IPCE(\%) \times LHE \quad (2)$$

where $LHE = 1 - 10^{-A}$, A is the absorbance according to the UV-vis spectrum.

Text S7. Calculation of ABPE

Applied bias photon-to-current efficiency (ABPE) can be calculated using the following equation:

$$ABPE(\%) = \frac{J \times (1.23 - V_b)}{P} \times 100\% \quad (3)$$

where J is the photocurrent density ($mA \cdot cm^{-2}$) obtained from the electrochemical workstation. V_b refers to the applied bias versus RHE (V), and P is the total light intensity of AM 1.5 G (100 $mV \cdot cm^{-2}$).

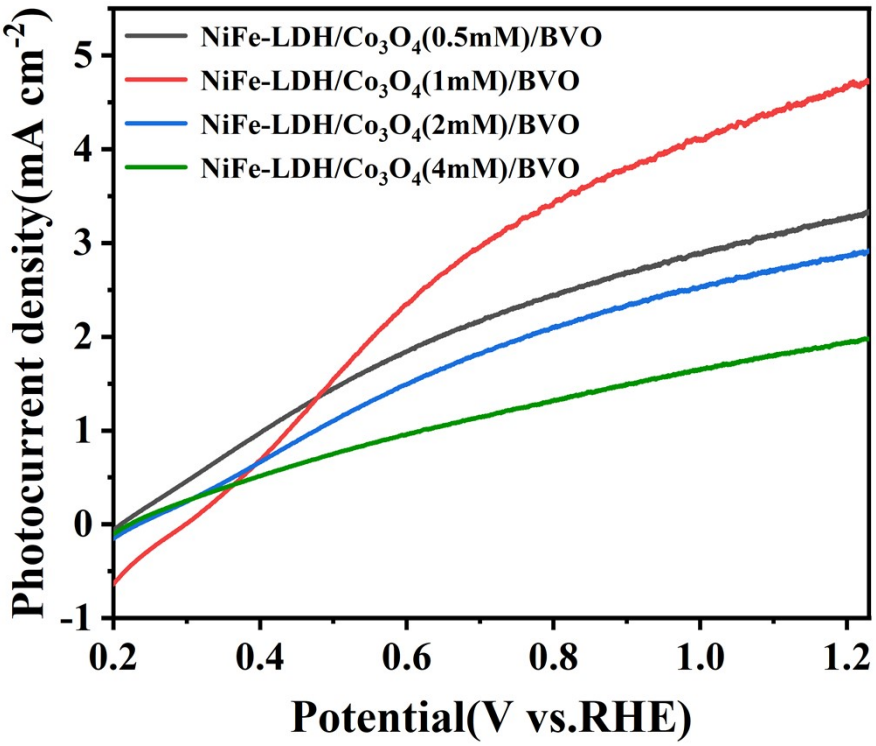

S1. LSV curves of NiFe-LDH/Co_3O_4/$BiVO_4$ photoanodes at different cobalt contents in 1.0M KBi electrolyte (pH=9.5) under AM 1.5 G illumination (100 mW cm^{-2}).

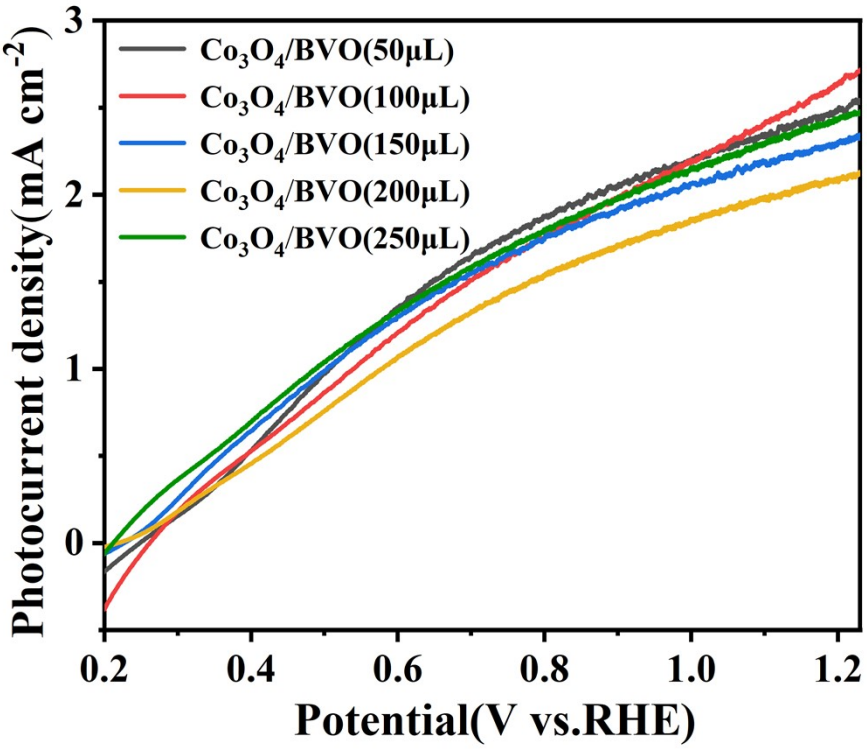

S2. LSV curves of NiFe-LDH/Co_3O_4/$BiVO_4$ photoanodes at different Co_3O_4 loadings in 1.0 M KBi electrolyte (pH=9.5) under AM 1.5 G illumination (100 mW cm^{-2}).

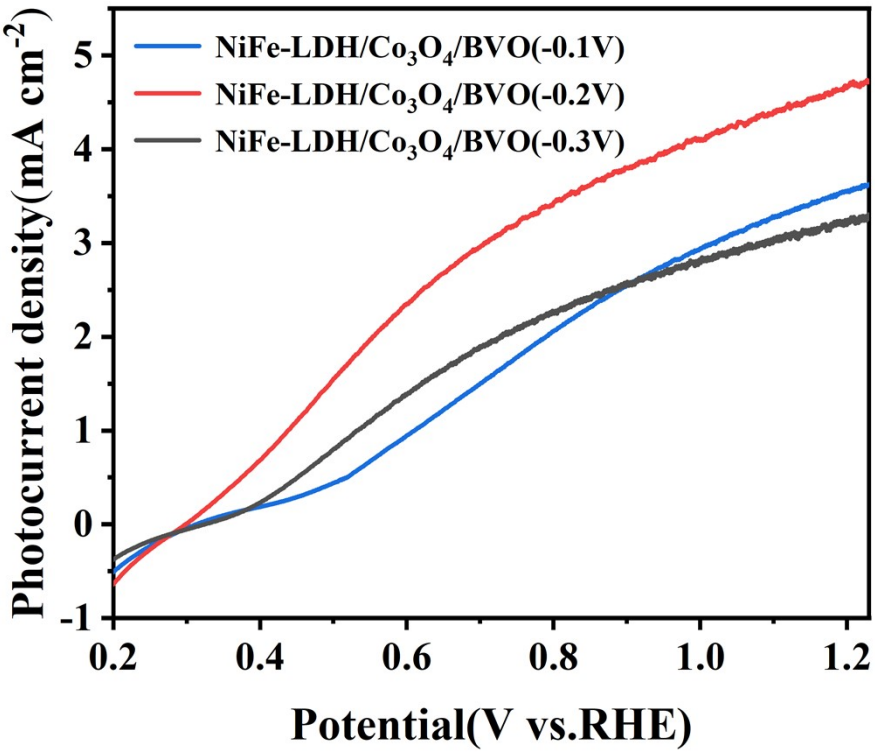

S3. LSV curves of NiFe-LDH in NiFe-LDH/Co_3O_4/$BiVO_4$ photoanodes with different deposition voltages.

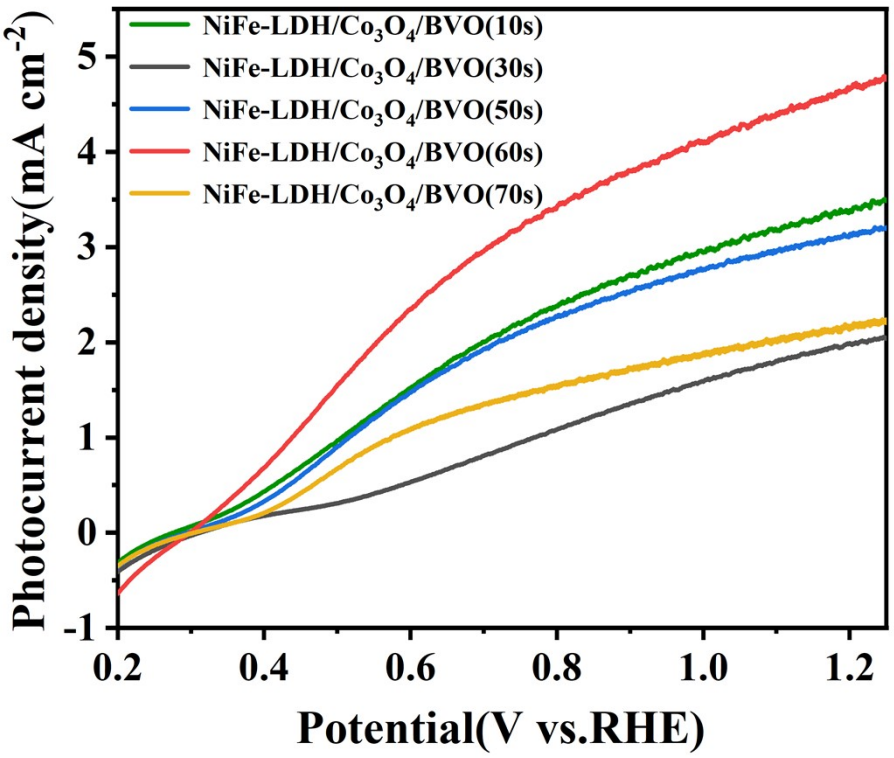

S4. LSV curves of NiFe-LDH in NiFe-LDH/Co_3O_4/$BiVO_4$ photoanodes with different deposition time.

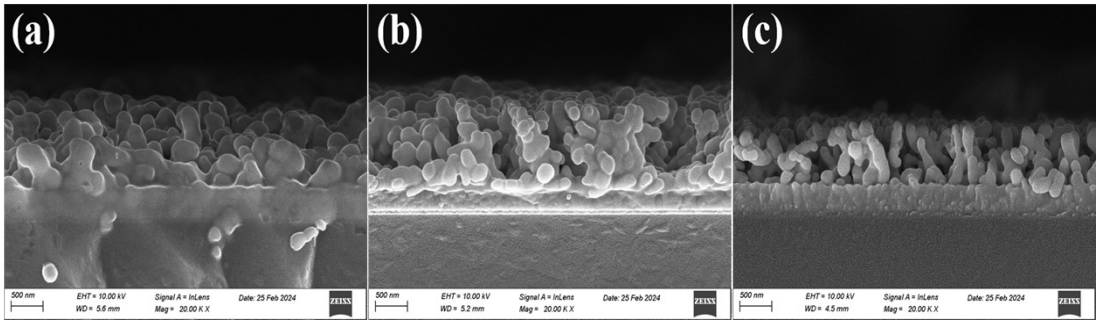

S5. SEM cross-sectional images of (a) $BiVO_4$, (b) Co_3O_4/$BiVO_4$, and (c) NiFe-LDH/Co_3O_4/$BiVO_4$ films.

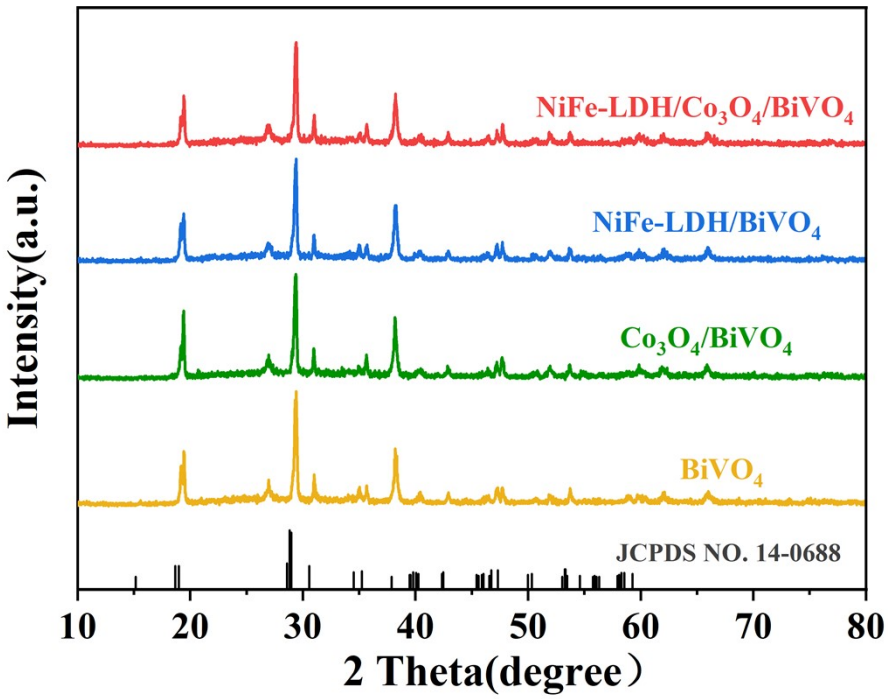

S6. XRD pattern of $BiVO_4$, $Co_3O_4/BiVO_4$, NiFe-LDH/$BiVO_4$ and NiFe-LDH/$Co_3O_4/BiVO_4$.

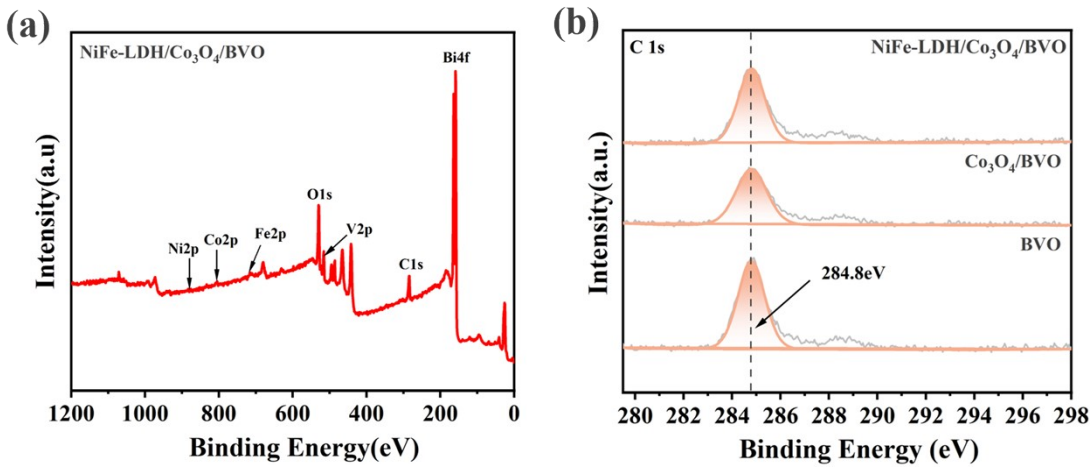

S7. The XPS spectrum of (a) survey and (b) C 1s.

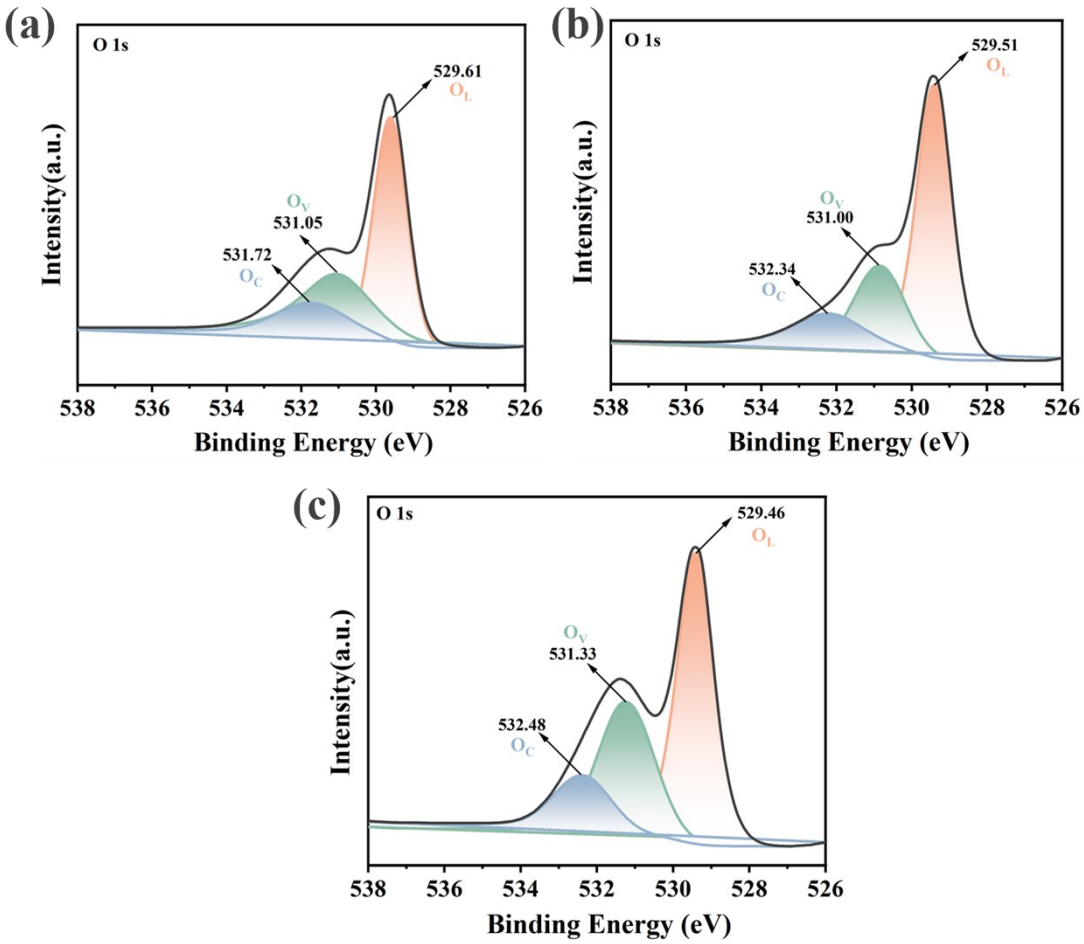

S8. The XPS O 1s spectrum of $BiVO_4$, $Co_3O_4/BiVO_4$ and NiFe-LDH/$Co_3O_4/BiVO_4$.

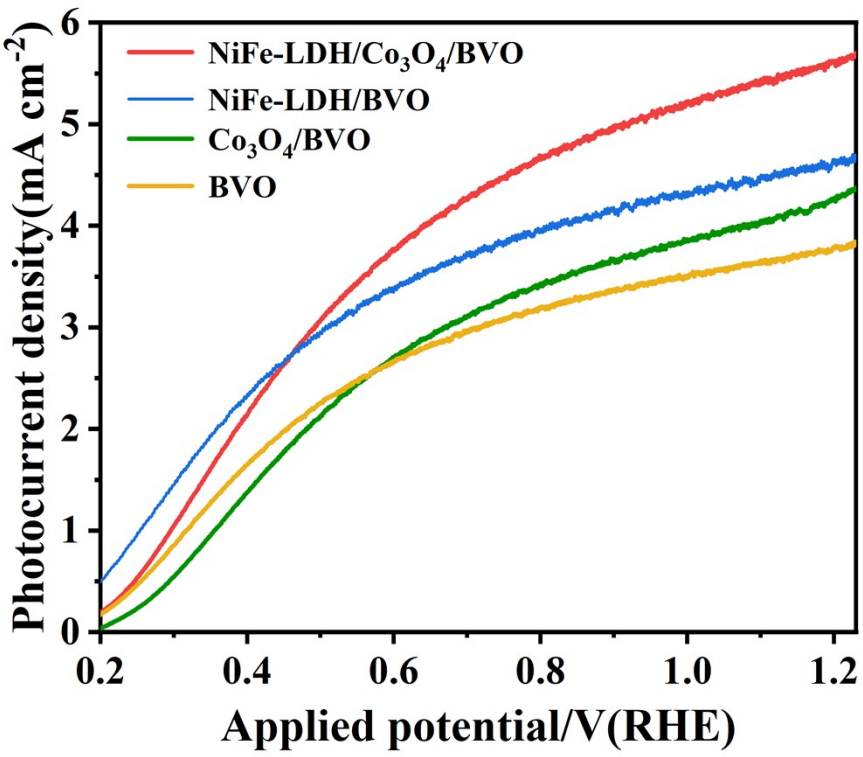

S9. LSV curves in the presence of 1 M Na_2SO_3 with a scan rate of 50 mV s^{-1}.

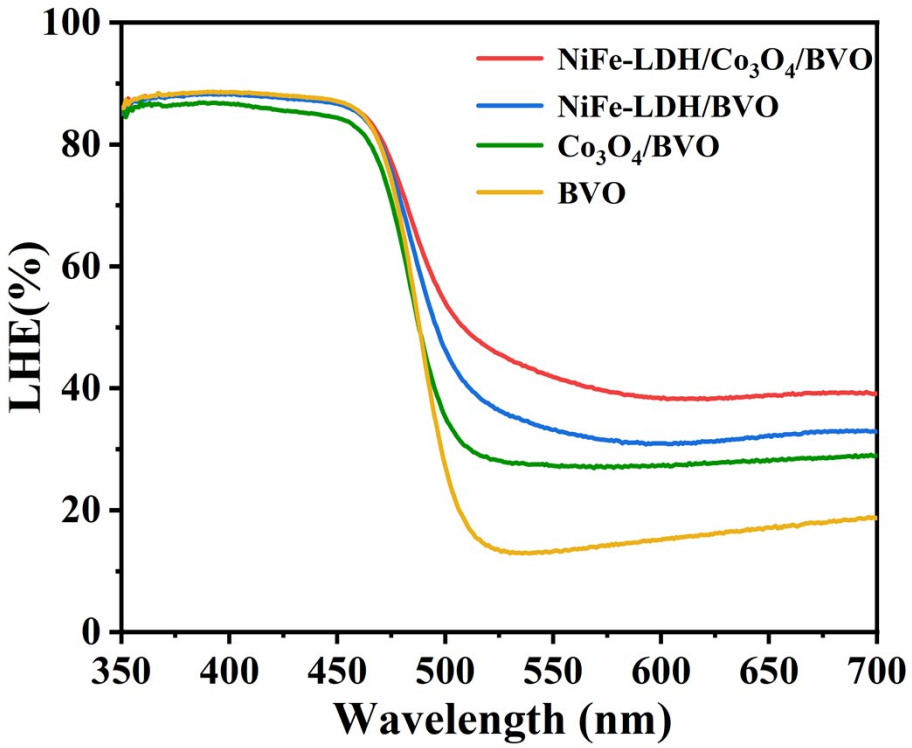

S10. LHE (Light harvesting efficiency) of all samples.

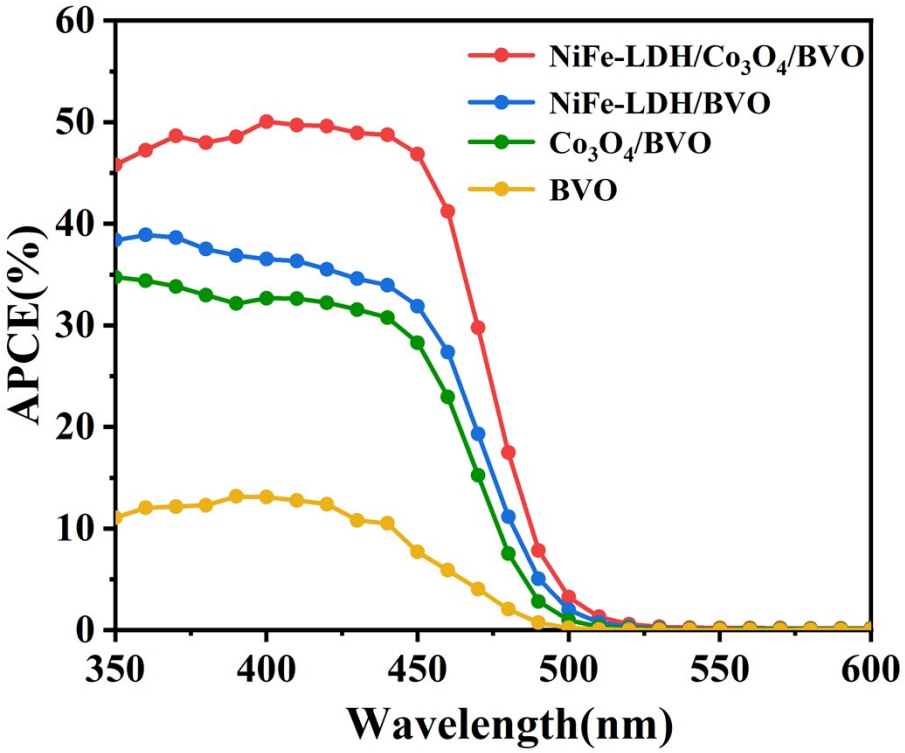

S11. APCE (absorption photon-current efficiency) of all samples.

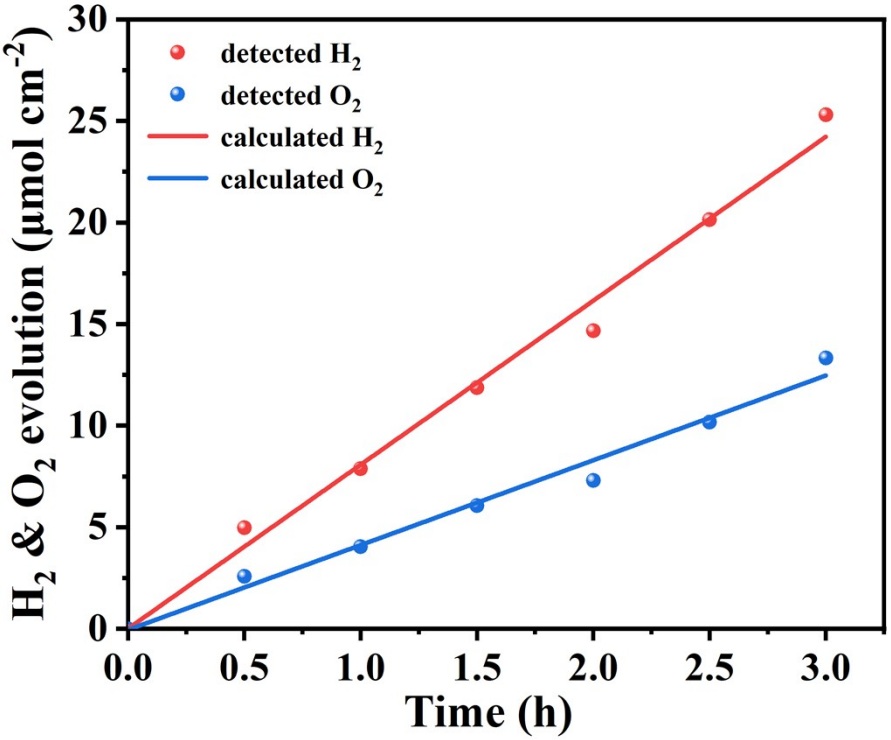

S12. H_2 and O_2 evolution of $BiVO_4$ photoanode at 1.23V vs. RHE under AM1.5G illumination.

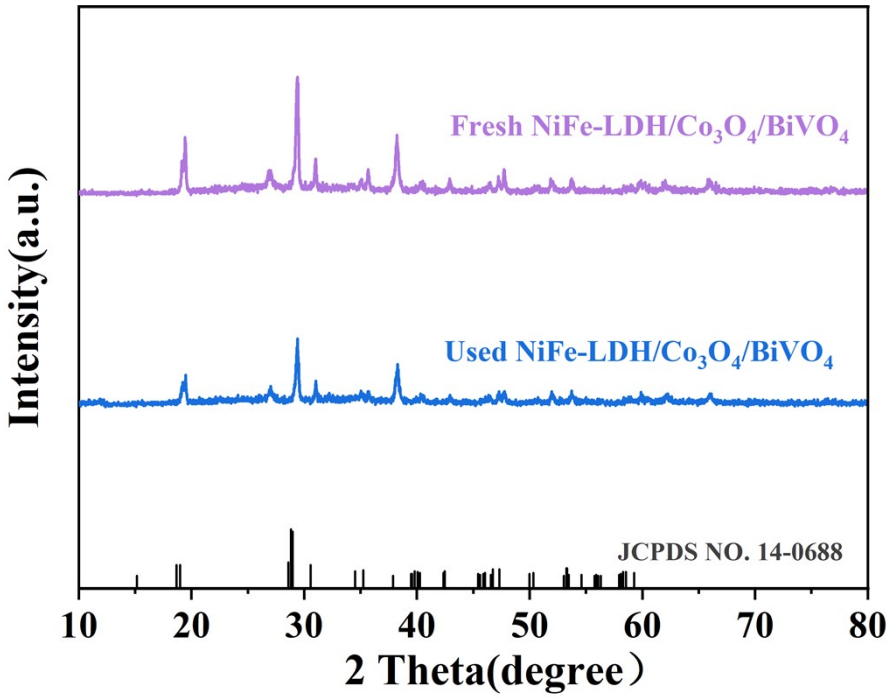

S13. XRD patterns of NiFe-LDH/Co_3O_4/$BiVO_4$ photoanode before and after PEC measurements.

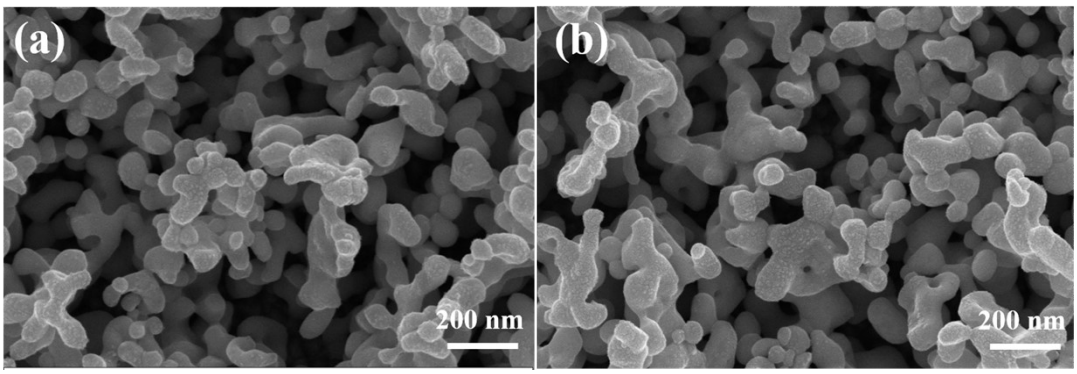

S14. SEM images of a NiFe-LDH/Co_3O_4/$BiVO_4$ film before (a) and after (b) the PEC measurements.

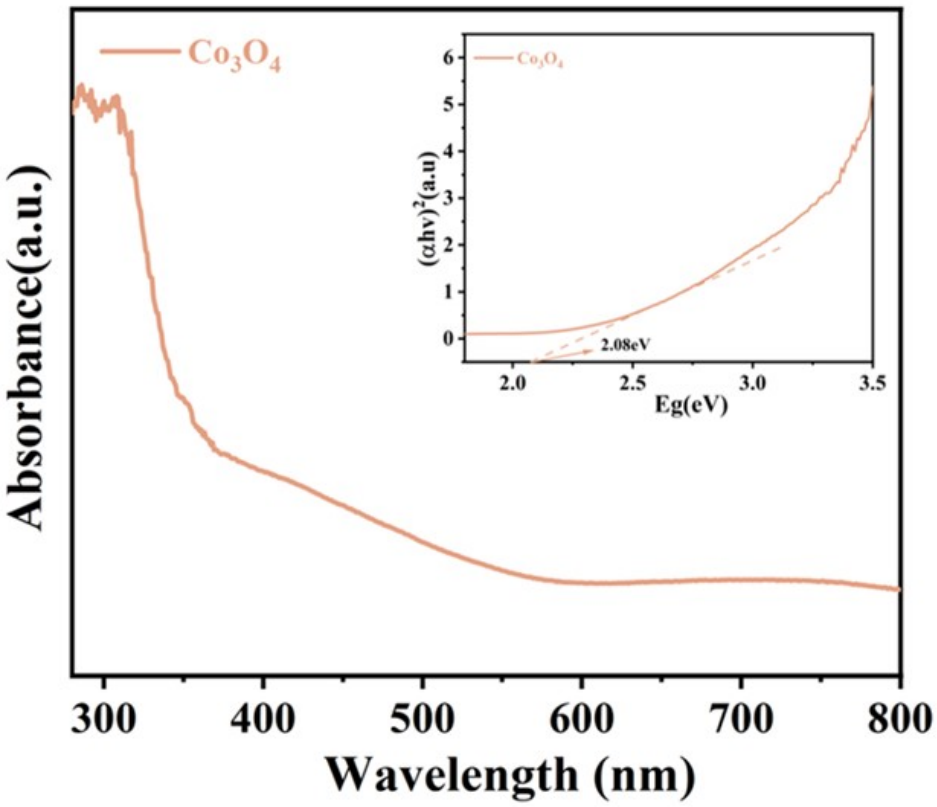

S15. UV-vis DRS spectra of Co_3O_4 along with its estimated band gap energy.

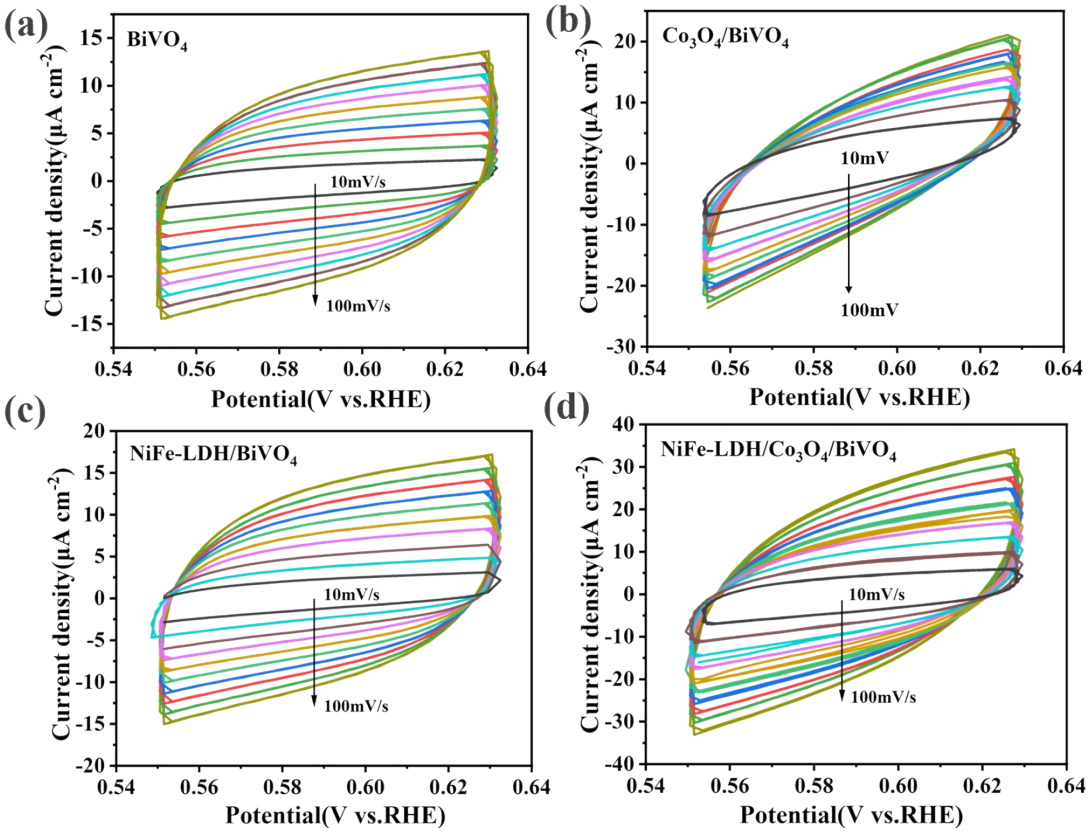

S16. Cyclic Voltammetry (CV) tests at different scanning rates of 10 ~ 100 mV s^{-1} for (a) $BiVO_4$, (b) $Co_3O_4/BiVO_4$, (c) NiFe-LDH/$BiVO_4$ and (d) NiFe-LDH/$Co_3O_4/BiVO_4$.

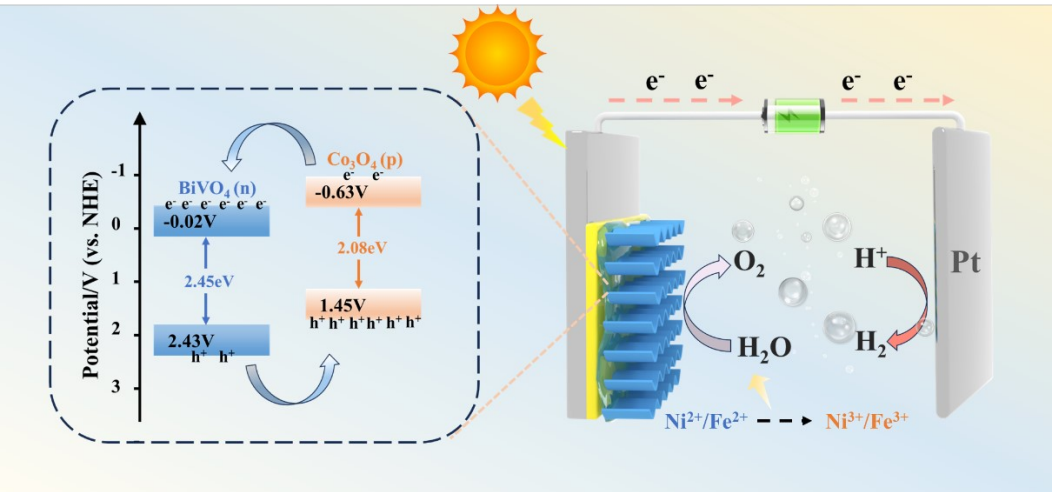

S17. Energy band alignment diagram of $Co_3O_4/BiVO_4$.

Table S1. Comparison of PEC performance of reported $BiVO_4$ photoanodes at 1.23V vs. RHE

Photoelectrode	Reaction conditions	Photocurrent	H_2/O_2	Ref.
NiFe-LDH/Co_3O_4/$BiVO_4$	1.0 M KBi AM 1.5G	4.7 mA/cm^2	55.7 μmol/h H_2 27.5 μmol/h O_2	This work
$BiVO_4$/NiFeOOH /Co-Pi	0.5 M Na_2SO_4 AM 1.5 G	2.03 mA/cm^2	7.0 μmol/h H_2 3.6 μmol/h O_2	[1]
$Ni(OH)_2$/Cl-$BiVO_4$	0.5 M K_3BO_3 AM 1.5 G	4.33 mA/cm^2	34.1 μmol/h H_2 16.5 μmol/h O_2	[2]
$BiVO_4$/BiOBr	0.5 M Na_2SO_4 AM 1.5 G	2.69 mA/cm^2	-	[3]
$BiVO_4$/Mn-NiOOH	0.5M Na_2SO_4 AM 1.5 G	2.41 mA/cm^2	-	[4]
$BiVO_4$/Al_2O_3(a)/FeOOH	1.0 M Na_2SO_3 AM 1.5 G	3.8 mA/cm^2	-	[5]
Nd:$BiVO_4$@NiCo-LDH	0.5M Na_2SO_4 AM 1.5 G	4.1 mA/cm^2	-	[6]
FeOOH/Ti:$BiVO_4$	0.2 M Na_2SO_4 AM 1.5 G	3.99 mA/cm^2	31.6 μmol/h H_2 15.5 μmol/h O_2	[7]

1. Fang, G.; Liu, Z.; Han, C., Enhancing the PEC water splitting performance of BiVO4 co-modifying with NiFeOOH and Co-Pi double layer cocatalysts. *Applied Surface Science* **2020,** *515*, 146095.
2. Zhang, J.; Wei, X.; Zhao, J.; Zhang, Y.; Wang, L.; Huang, J.; She, H.; Wang, Q., Electronegative Cl− modified BiVO4 photoanode synergized with nickel hydroxide cocatalyst for high-performance photoelectrochemical water splitting. *Chemical Engineering Journal* **2023,** *454*, 140081.
3. Shuai, L.; Tian, L.; Huang, X.; Dou, J.; Yu, J.; Chen, X., Enhanced charge carrier separation and stable photoelectrochemical water splitting via a high-performance BiVO4/BiOBr Type-II heterojunction. *International Journal of Hydrogen Energy* **2024,** *88*, 19-28.
4. Soundarya Mary, A.; Murugan, C.; Mahendiran, D.; Murugan, P.; Pandikumar, A., Investigation of Mn incorporation into NiOOH electrocatalyst loaded on BiVO4 photoanode for enhanced photoelectrochemical water splitting: Experimental and theoretical approach. *Materials Today Energy* **2024,** *41*, 101541.
5. Yang, J.; Tao, Z.; Zhao, Q.; Li, J.; Liu, G., Synergistic effect of FeOOH cocatalyst and Al2O3 passivation layer on BiVO4 photoanode for enhanced photoelectrochemical water oxidation. *Journal of Alloys and Compounds* **2025,** *1010*, 177461.
6. Wang, M.; Wu, L.; Geng, L.; Gao, L.; Ge, J.; Niu, H.; Li, H.; Jin, J., Bifunctional NiCo-LDH cocatalyst with hole extraction and high catalytic activity for boosting photoelectrochemical water oxidation of Nd doped BiVO4 photoanode. *Journal of Alloys and Compounds* **2024,** *987*, 174183.
7. Wang, J.; Bai, J.; Zhang, Y.; Li, L.; Zhou, C.; Zhou, T.; Li, J.; Zhu, H.; Zhou, B., Unconventional Substitution for BiVO4 to Enhance Photoelectrocatalytic Performance by Accelerating Polaron Hopping. *ACS Applied Materials & Interfaces* **2023,** *15* (11), 14359-14368.